ANALYSIS OF OUTAGE PROBABILITY AND INTERCEPT PROBABILITY TRADE-OFF FOR SECURE TWO-WAY RELAYING SCHEMES BETWEEN TWO CLUSTERS OF NODES USING FOUNTAIN CODES

Thi-Hau Nguyen[1,2], *Minh Nam Pham*[1], *Tran Trung Duy*[3,*], *Lam-Thanh Tu*[4], *Khuong Ho-Van*[5,6]

Abstract

This paper presents two secure two-way relaying schemes between two clusters of nodes: i) 3-phase two-way relaying using Digital Network Coding; ii) conventional 4-phase two-way relaying. In the proposed schemes, one node selected from each cluster will use Fountain codes to encode the original data, and then send encoded packets to nodes in the remaining cluster, with the help of a common relay node. Explicit mathematical expressions are derived to evaluate the outage probability (system outage probability) and intercept probability (system intercept probability) of the proposed schemes over the Rayleigh fading channel. Our results show a reliability-security trade-off as well as the impact of system parameters on the network performances.

Index terms

Two-way relaying networks; digital network coding; physical-layer security; Fountain codes; outage probability; intercept probability.

1. Introduction

Two-way relaying network (TWRN) [1] is one of efficient solutions in wireless communication networks, where two source nodes wish to exchange their data with

[1]Faculty of Electronics Technology, Industrial University of Ho Chi Minh City
[2]Faculty of Electronics and Telecommunications, Saigon University
[3]Faculty of Telecommunications 2, Posts and Telecommunications Institute of Technology
[4]Faculty of Electrical and Electronics Engineering, Ton Duc Thang University
[5]Faculty of Electrical and Electronics Engineering, Ho Chi Minh City University of Technology (HCMUT)
[6]Vietnam National University Ho Chi Minh City
[*]Corresponding author, email: trantrungduy@ptithcm.edu.vn DOI:10.56651/lqdtu.jst.v13.n02.927.ict

each other with the assistance of intermediate relay nodes. Conventionally, exchanging data between two sources is performed in four phases, in which one source sends its data to the remaining one in each two phases. Consequently, the achievable transmission rate is 2 packets/4 phases [1]. To enhance the data rate, new Two-way relaying (TWR) models that reduce the number of transmission phases are proposed. In [1]–[3], Digital Network Coding (DNC) technique is employed at the relay node to reduce 1 phase, thereby achieving a transmission rate of 2 packets/3 phases. The work [4] proposes a combination of Successive Interference Cancellation and DNC technique at the relay node to achieve a transmission rate of 2 packets/2 phases. TWRN schemes proposed in [5], [6] reach a transmission rate of 2 packets/1 phase provided that source nodes and relay nodes are equipped with multiple antennas and operate in full-duplex mode. Since interference cancellation operation at the nodes [5], [6] are very complex, this paper only studies the DNC-aided 3-phase and 4-phase TWR schemes.

Physical-Layer Security (PLS) [7], [8] is a simple and potential security technique. In [9], the PLS with Randomize and Forward (RF) technique is proposed to reduce the overhearing possibility of the eavesdropper. This technique is widely employed in the PLS relaying networks [10], [11], in which the trade-off between the reliability $(\mathrm{OP}$: Outage Probability) and security $(\mathrm{IP}$: Intercept Probability) is investigated. In [12], [13], the PLS schemes using Artificial Noise Generating (ANG) are proposed and analyzed. However, implementing ANG is complex due to high synchronization requirements among nodes. Recently, the combination of the TWR and PLS schemes has been introduced in [14]–[16]. In [14], the authors evaluate the secure outage probability performance of the TWRPLS schemes using ANG. In [15], [16], the TWRPLS schemes employing Intelligent Reflecting Surface have been studied. Unlike [14]–[16], this paper studies TWRPLS scheme using Fountain Codes (FCs).

FCs [17] is widely applied in wireless networks due to its high adaptability to channel variations, simplicity in design, and ability to prevent re-transmission of a single packet from transmitters to receivers when transmission errors occur. The FCs transmitter generates encoded packets continuously, then transmit them to the receivers, which attempt to gather sufficient packets for data recovery [10], regardless of the specific packets received. As a result, it avoids feedback from the receivers to the transmitter for the retransmission. As proven in [18], using FCs significantly reduces delay time, as compared with the conventional transmission method, especially in broadcast networks. Recently, combination between FCs and PLS has been gained much attention. In the PLS schemes using FCs [19], [20], it is proved that the data transmission is reliable and secure when the legitimate receivers collect sufficient packets and the eavesdroppers cannot. Published work [21] studies the trade-off between OP and IP for multicast PLS schemes. In [22], the $\mathrm{OP}-\mathrm{IP}$ trade-off for hybrid satellite-terrestrial relaying networks using FCs is investigated.

This paper studies the secure 4-phase and DNC-aided 3-phase TWR schemes between two clusters of nodes using FCs. Main contributions of this paper are:

- Propose two new TWR schemes to enhance the performance with low implementation complexity, reduced delay, high reliability, and ensuring information security.

- Derive exact closed-form expressions of OP, IP, SOP (System OP), and SIP (System IP) of the proposed schemes over Rayleigh fading channels. The derived expressions are verified by Monte-Carlo simulations. It is worth noting that the derived expressions can be effectively utilized for system design and optimization.
- Derive approximate expressions of OP in the high SNR (Signal-to-Noise Ratio) regions. These approximate expressions prove that all the considered schemes obtain the same OP slope.

The rest of this paper is provided as follows: the system model of the proposed schemes is presented in Section 2; Section 3 analyzes OP, IP, SOP, and SIP performance; Section 4 provides the simulation and theoretical results; Section 5 concludes this paper and proposes future development directions.

2. System model

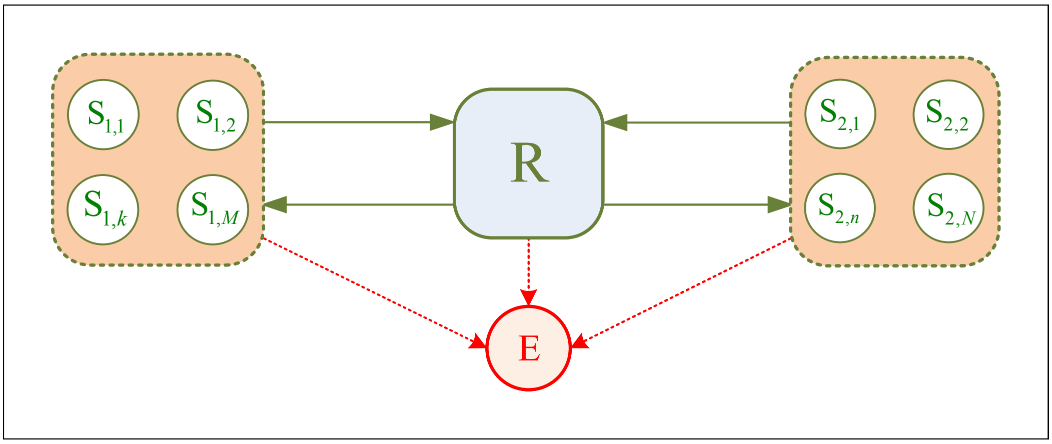

Fig. 1. Proposed secure TWR scheme.

Fig. 1 depicts the secure TWRN scheme between two clusters of nodes. Assume that the first cluster has M nodes, denoted by $\mathrm{S}_{1,1}, \mathrm{S}_{1,2}..., \mathrm{S}_{1,M}$, and the second one has N nodes, denoted by $\mathrm{S}_{2,1}, \mathrm{S}_{2,2}..., \mathrm{S}_{2,N}$, where $M \geq 2$, $N \geq 2$. In each cluster, a cluster node is randomly selected to send its data to the nodes in the remaining cluster. The selected nodes in the first and second clusters are denoted by S_1 and S_2, respectively. Data from S_1 and S_2 are denoted as m_1 and m_2, respectively. It is assumed that two clusters cannot directly communicate, and hence S_1 and S_2 have to exchange their data via the assistance of a common relay R. In Fig. 1, an eavesdropper (E) illegally listens and decodes the m_1 and m_2 data. Assume that the nodes $\mathrm{S}_{1,k}$, $\mathrm{S}_{2,n}$, R, and E are equipped with one transmit antenna and one receive antenna, and operate in a half-duplex mode, where $k = 1, 2, ..., M$, $n = 1, 2, ..., N$.

Using FCs, $\mathrm{S}_1\,(\mathrm{S}_2)$ encodes $m_1\,(m_2)$ to create encoded packets (or Fountain packets) that are denoted by $p_1\,(p_2)$. m_1 and m_2 will exchange their Fountain packets with each other via R. To correctly reconstruct $m_1\,(m_2)$,$\mathrm{S}_{1,k}$, $\mathrm{S}_{2,n}$, and E must receive at least $H_{\min}$ packets $p_1\,(p_2)$ [10]. Additionally, due to a delay constraint, the maximum number of exchanging the encoded packets is limited by $N_{\max}$, where $N_{\max} \geq H_{\min}$. It is noted that E can receive $p_1\,(p_2)$ from both R and $\mathrm{S}_1\,(\mathrm{S}_2)$. To reduce overhearing possibility of E, the RF technique [9]–[11] is hence employed by $\mathrm{S}_1\,(\mathrm{S}_2)$ and R.

This paper studies two TWR schemes, i.e., 3-phase TWR using DNC (named $\mathrm{TWR}-3\mathrm{P}$) and conventional 4-phase TWR (named $\mathrm{TWR}-4\mathrm{P}$). In the $\mathrm{TWR}-4\mathrm{P}$ scheme, S_1 sends p_1 to R in the first phase. Next, R decodes p_1, re-encodes, and sends p_1 to the nodes in the second cluster in the second phase. Similarly, p_2 is sent from S_2 to R, afterwards R decodes and forwards p_2 to the first cluster in the third and fourth phases, respectively. In the $\mathrm{TWR}-3\mathrm{P}$ scheme, S_1 and S_2 send p_1 and p_2 to R in the first phase and the second phase, respectively. If R decodes both p_1 and p_2 successfully, it performs the R operation on p_1 and p_2, i.e., $p_\oplus = p_1 \oplus p_2$. Then, it broadcasts $p_\oplus$ to two clusters in the third phase. Considering the node $\mathrm{S}_{1,k}$ ($\mathrm{S}_{1,k} \neq \mathrm{S}_1$), when S_1 sends p_1 to R, $\mathrm{S}_{1,k}$ can also receive p_1. Assume that $\mathrm{S}_{1,k}$ always decodes p_1 successfully from S_1 due to the short distance between them. If $\mathrm{S}_{1,k}$ can decode $p_\oplus$ from R correctly, it can obtain p_2 by performing the XOR operation on p_1 and $p_\oplus$, i.e., $p_\oplus \oplus p_1 = p_2$. Similarly, if $\mathrm{S}_{2,n}$ decodes $p_\oplus$ correctly, it can correctly obtain p_1 by performing the XOR operation on p_2 and $p_\oplus$.

Let us consider the case where R only decodes p_1(or p_2) successfully. In this case, it only sends p_1(or p_2) to the second cluster (or the first cluster) in the third phase. If neither p_1 nor p_2 is decoded correctly, R will do nothing in the third phase.

Considering the node E in the $\mathrm{TWR}-3\mathrm{P}$ scheme; if E can decode both p_1 and p_2 correctly in the first and second phases, respectively, it does not need to decode $p_\oplus$ any more. On the other hand, if E can decode p_1 successfully, but cannot decode p_2 successfully, it tries to decode $p_\oplus$ from R. Afterwards, E can obtain p_2 by performing the operation on $p_\oplus$ and p_1. Similarly, if E can decode p_2 but cannot decode p_1, it can obtain p_1 if the decoding of $p_\oplus$ is successful.

Let g_{TxRx} denote channel gain between Tx and Rx, CDF (Cumulative Distribution Function) and PDF (Probability Density Function) of g_{TxRx} is given, respectively as

$$\begin{aligned} &F_{g_{\mathrm{TxRx}}}(x) = 1 - \exp\left(-\lambda_{\mathrm{TxRx}} x\right), \\ &f_{g_{\mathrm{TxRx}}}(x) = \lambda_{\mathrm{TxRx}} \exp\left(-\lambda_{\mathrm{TxRx}} x\right), \end{aligned} \tag{1}$$

where $F_X(x)$ and $f_X(x)$ are CDF and PDF of random variable X, $\lambda_{\mathrm{TxRx}} = (d_{\mathrm{TxRx}})^\beta$ [10], where d_{TxRx} is distance between Tx and Rx, and $\beta\,(2 \leq \beta \leq 6)$ is the path-loss factor. It is assumed that the nodes in one cluster are close together, hence $d_{\mathrm{S}_{1,k}\mathrm{R}} = d_{\mathrm{S}_1\mathrm{R}}$ (or $\lambda_{\mathrm{S}_{1,k}\mathrm{R}} = \lambda_{\mathrm{S}_1\mathrm{R}}$), $d_{\mathrm{S}_{2,n}\mathrm{R}} = d_{\mathrm{S}_2\mathrm{R}}$ (or $\lambda_{\mathrm{S}_{2,n}\mathrm{R}} = \lambda_{\mathrm{S}_2\mathrm{R}}$), $d_{\mathrm{S}_{1,k}\mathrm{E}} = d_{\mathrm{S}_1\mathrm{E}}$ (or $\lambda_{\mathrm{S}_{1,k}\mathrm{E}} = \lambda_{\mathrm{S}_1\mathrm{E}}$), and $d_{\mathrm{S}_{2,n}\mathrm{E}} = d_{\mathrm{S}_2\mathrm{E}}$ (or $\lambda_{\mathrm{S}_{2,n}\mathrm{E}} = \lambda_{\mathrm{S}_2\mathrm{E}}$) for $\forall k, n$.

Next, the instantaneous SNR of the $\mathrm{Tx} \to \mathrm{Rx}$ link is written as

$$\gamma_{\mathrm{TxRx}} = \frac{P_{\mathrm{Tx}} g_{\mathrm{TxRx}}}{\sigma_{\mathrm{Rx}}^2}, \tag{2}$$

where P_{Tx}, and σ_{Rx}^2 are the transmit power of Tx and the variance of Gaussian noise at Rx. Assume that S_1, S_2, and R are the same types (e.g., sensor nodes). Hence their transmit power is assumed to be the same ($P_{\mathrm{S}_1} = P_{\mathrm{S}_2} = P_{\mathrm{R}} = P$).
It is also assumed that the variance of Gaussian noise is identical ($\sigma_{\mathrm{RX}}^2 = \sigma_0^2$) for $\forall \mathrm{Rx} \in \{\mathrm{S}_{1,k}, \mathrm{S}_1, \mathrm{S}_{2,n}, \mathrm{S}_2, \mathrm{R}, \mathrm{E}\}$.

Then, the instantaneous channel capacity of the $\mathrm{Tx} \to \mathrm{Rx}$ link in the $\mathrm{TWR}-3\mathrm{P}$ scheme and the $\mathrm{TWR}-4\mathrm{P}$ scheme can be formulated, respectively as

$$C_{\mathrm{TxRx}}^{\mathrm{TWR}-3\mathrm{P}} = \frac{1}{3}\log_2\left(1+\gamma_{\mathrm{TxRx}}\right) = \frac{1}{3}\log_2\left(1+\Delta g_{\mathrm{TxRx}}\right), \tag{3}$$

$$C_{\mathrm{TxRx}}^{\mathrm{TWR}-4\mathrm{P}} = \frac{1}{4}\log_2\left(1+\gamma_{\mathrm{TxRx}}\right) = \frac{1}{4}\log_2\left(1+\Delta g_{\mathrm{TxRx}}\right), \tag{4}$$

where $\Delta = P/\sigma_0^2$; the factor $1/3$ and $1/4$ indicate that the packet exchange in $\mathrm{TWR}-3\mathrm{P}$ and $\mathrm{TWR}-4\mathrm{P}$ is performed over 3 phases and 4 phases, respectively.

Assume that $p_j\,(j=1,2)$ can be correctly decoded by Rx if $C_{\mathrm{TxRx}}^{\mathrm{Z}} \geq C_{\mathrm{th}}$, where $Z \in \{\mathrm{TWR}-3\mathrm{P}, \mathrm{TWR}-4\mathrm{P}\}$ and C_{th} is a predetermined target rate.

3. Performance analysis

This section derives exact closed-form expressions of OP(SOP) and IP(SIP) for two proposed schemes. Particularly, OP of the first cluster (the second cluster) is defined as the probability that all the nodes of the first cluster (the second cluster) cannot collect at least $H_{\min}$ Fountain packets to recover the desired data. Next, IP with respect to the data $m_j\,(j=1,2)$, is defined as the probability that E can receive correctly at least $H_{\min}$ packets p_j. For the system performance, SOP is the probability that at least one of two clusters is outage while SIP is the probability that at least one of two data m_1 or m_2 is intercepted.

3.1. Performance analysis for TWR-4P

3.1.1. OP and SOP: First, let us consider OP of the second cluster (denoted by $\mathrm{OP}_2^{\mathrm{TWR}-4\mathrm{P}}$). Let $L_{2,n}$ denote the number of encoded packets p_1 decoded correctly by $\mathrm{S}_{2,n}$. Then, the second cluster is outage if $L_{2,n} < H_{\min}$ for $\forall n$. U_1 is denoted as the number of encoded packets p_1 decoded correctly by R after the data exchange ends. As a result, $N_{\max} - U_1$ is the number of encoded packets p_1 decoded unsuccessfully by R, (or $N_{\max} - U_1$ is the number of encoded packets p_1 decoded unsuccessfully by R).

Case 1: $0 \leq U_1 < H_{\min}$

Because $U_1 < H_{\min}$, this means that there are no nodes in the second cluster can receive enough $H_{\min}$ packets p_1, and hence the second cluster is outage. Using (1)-(4), the OP of the second cluster in this case can be written as

$$\begin{aligned}\mathrm{OP}_{2,\mathrm{TH1}}^{\mathrm{TWR-4P}} &= \sum_{U_1=0}^{H_{\min}-1} C_{N_{\max}}^{U_1}\left[\Pr\left(C_{\mathrm{S_1R}}^{\mathrm{TWR-4P}} \geq C_{\mathrm{th}}\right)\right]^{U_1}\left[\Pr\left(C_{\mathrm{S_1R}}^{\mathrm{TWR-4P}} < C_{\mathrm{th}}\right)\right]^{N_{\max}-U_1} \\ &= \sum_{U_1=0}^{H_{\min}-1} C_{N_{\max}}^{U_1}\exp\left(-U_1\lambda_{\mathrm{S_1R}}\rho_{\mathrm{th1}}\right)\left[1-\exp\left(-\lambda_{\mathrm{S_1R}}\rho_{\mathrm{th1}}\right)\right]^{N_{\max}-U_1}. \end{aligned} \tag{5}$$

where $C_{N_{\max}}^{U_1} = \frac{N_{\max}!}{U_1!(N_{\max}-U_1)!}$, $\rho_{\mathrm{th1}} = \left(2^{4C_{\mathrm{th}}}-1\right)/\Delta$.

Case 2: $H_{\min} \leq U_1 \leq N_{\max}$

In this case, OP of the second cluster can be formulated as

$$\begin{aligned}\mathrm{OP}_{2,\mathrm{TH2}}^{\mathrm{TWR-4P}} = \sum_{U_1=H_{\min}}^{N_{\max}} & C_{N_{\max}}^{U_1}\left[\Pr\left(C_{\mathrm{S_1R}}^{\mathrm{TWR-4P}} \geq C_{\mathrm{th}}\right)\right]^{U_1}\left[\Pr\left(C_{\mathrm{S_1R}}^{\mathrm{TWR-4P}} < C_{\mathrm{th}}\right)\right]^{N_{\max}-U_1} \\ & \times \prod_{n=1}^{N}\Pr\left(L_{2,n} < H_{\min}|U_1\right), \end{aligned} \tag{6}$$

where $\Pr\left(L_{2,n} < H_{\min}|U_1\right)$ is probability that $\mathrm{S}_{2,n}$ cannot collect enough encoded packets p_1, and this probability can be formulated as

$$\begin{aligned}&\Pr\left(L_{2,n} < H_{\min}|U_1\right) = \\ &\sum_{L_{2,n}=0}^{H_{\min}-1} C_{U_1}^{L_{2,n}}\left[\Pr\left(C_{\mathrm{RS}_{2,n}}^{\mathrm{TWR-4P}} \geq C_{\mathrm{th}}\right)\right]^{L_{2,n}}\left[\Pr\left(C_{\mathrm{RS}_{2,n}}^{\mathrm{TWR-4P}} < C_{\mathrm{th}}\right)\right]^{U_1-L_{2,n}}. \end{aligned} \tag{7}$$

Similar to (5), using (1)-(4), $\mathrm{OP}_{2,\mathrm{TH2}}^{\mathrm{TWR-4P}}$ can be given as

$$\begin{aligned}\mathrm{OP}_{2,\mathrm{TH2}}^{\mathrm{TWR-4P}} &= \sum_{U_1=H_{\min}}^{N_{\max}} C_{N_{\max}}^{U_1}\exp\left(-U_1\lambda_{\mathrm{S_1R}}\rho_{\mathrm{th1}}\right)\left[1-\exp\left(-\lambda_{\mathrm{S_1R}}\rho_{\mathrm{th1}}\right)\right]^{N_{\max}-U_1} \\ \times & \left\{\sum_{L_{2,n}=0}^{H_{\min}-1} C_{U_1}^{L_{2,n}}\exp\left(-L_{2,n}\lambda_{\mathrm{RS_2}}\rho_{\mathrm{th1}}\right)\left[1-\exp\left(-\lambda_{\mathrm{RS_2}}\rho_{\mathrm{th1}}\right)\right]^{U_1-L_{2,n}}\right\}^{N}. \end{aligned} \tag{8}$$

Combining (5) and (8), $\mathrm{OP}_{2}^{\mathrm{TWR-4P}}$ of the second cluster is presented as

$$\begin{aligned}\mathrm{OP}_{2}^{\mathrm{TWR-4P}} &= \mathrm{OP}_{2,\mathrm{TH1}}^{\mathrm{TWR-4P}} + \mathrm{OP}_{2,\mathrm{TH2}}^{\mathrm{TWR-4P}} \\ &= \sum_{U_1=0}^{H_{\min}-1} C_{N_{\max}}^{U_1}\exp\left(-U_1\lambda_{\mathrm{S_1R}}\rho_{\mathrm{th1}}\right)\left[1-\exp\left(-\lambda_{\mathrm{S_1R}}\rho_{\mathrm{th1}}\right)\right]^{N_{\max}-U_1}\end{aligned}$$

$$+\sum_{U_1=H_{\min}}^{N_{\max}} C_{N_{\max}}^{U_1} \exp\left(-U_1 \lambda_{\mathrm{S_1R}} \rho_{\mathrm{th1}}\right)\left[1-\exp\left(-\lambda_{\mathrm{S_1R}} \rho_{\mathrm{th1}}\right)\right]^{N_{\max}-U_1}$$
$$\times\left\{\sum_{L_{2,n}=0}^{H_{\min}-1} C_{U_1}^{L_{2,n}} \exp\left(-L_{2,n} \lambda_{\mathrm{S_2R}} \rho_{\mathrm{th1}}\right)\left[1-\exp\left(-\lambda_{\mathrm{S_2R}} \rho_{\mathrm{th1}}\right)\right]^{U_1-L_{2,n}}\right\}^N . \tag{9}$$

With the same derivation method, OP of the first cluster (denoted by $\mathrm{OP}_1^{\mathrm{TWR-4P}}$) can be computed as

$$\mathrm{OP}_1^{\mathrm{TWR-4P}}=\sum_{U_2=0}^{H_{\min}-1} C_{N_{\max}}^{U_2} \exp\left(-U_2 \lambda_{\mathrm{S_2R}} \rho_{\mathrm{th1}}\right)\left[1-\exp\left(-\lambda_{\mathrm{S_2R}} \rho_{\mathrm{th1}}\right)\right]^{N_{\max}-U_2}$$
$$+\sum_{U_2=H_{\min}}^{N_{\max}} C_{N_{\max}}^{U_2} \exp\left(-U_2 \lambda_{\mathrm{S_2R}} \rho_{\mathrm{th1}}\right)\left[1-\exp\left(-\lambda_{\mathrm{S_2R}} \rho_{\mathrm{th1}}\right)\right]^{N_{\max}-U_2}$$
$$\times\left\{\sum_{L_{1,k}=0}^{H_{\min}-1} C_{U_2}^{L_{1,k}} \exp\left(-L_{1,k} \lambda_{\mathrm{RS_1}} \rho_{\mathrm{th1}}\right)\left[1-\exp\left(-\lambda_{\mathrm{RS_1}} \rho_{\mathrm{th1}}\right)\right]^{U_2-L_{1,k}}\right\}^M . \tag{10}$$

However, expressions of $\mathrm{OP}_1^{\mathrm{TWR-4P}}$ and $\mathrm{OP}_2^{\mathrm{TWR-4P}}$ in (9) and (10) are still complex. This motivates us to find the approximate ones at the high SNR, i.e., $\Delta \rightarrow +\infty$. At first, using $1-\exp(-x) \overset{x \rightarrow 0}{\approx} x$, the $\mathrm{OP}_2^{\mathrm{TWR-4P}}$ in (9) can be approximated as

$$\mathrm{OP}_2^{\mathrm{TWR-4P}} \overset{\Delta \rightarrow +\infty}{\approx} C_{N_{\max}}^{H_{\min}-1}\left(\lambda_{\mathrm{S_1R}} \rho_{\mathrm{th1}}\right)^{N_{\max}+1-H_{\min}} . \tag{11}$$

Expression (11) also shows that the slope of $\mathrm{OP}_2^{\mathrm{TWR-4P}}$ equals to $N_{\max}+1-H_{\min}$:

$$\mathrm{D}_2^{\mathrm{TWR-4P}}=-\lim_{\Delta \rightarrow +\infty} \frac{\log\left(\mathrm{OP}_2^{\mathrm{TWR-4P}}\right)}{\log(\Delta)}=N_{\max}+1-H_{\min} . \tag{12}$$

Similarly, the approximate $\mathrm{OP}_1^{\mathrm{TWR-4P}}$ and the slope of $\mathrm{OP}_1^{\mathrm{TWR-4P}}$ can be expressed, respectively as

$$\mathrm{OP}_1^{\mathrm{TWR-4P}} \overset{\Delta \rightarrow +\infty}{\approx} C_{N_{\max}}^{H_{\min}-1}\left(\lambda_{\mathrm{S_2R}} \rho_{\mathrm{th1}}\right)^{N_{\max}+1-H_{\min}}, \mathrm{D}_1^{\mathrm{TWR-4P}}=N_{\max}+1-H_{\min} . \tag{13}$$

The (12) and (13) show that the slopes of $\mathrm{OP}_1^{\mathrm{TWR-4P}}$ and $\mathrm{OP}_2^{\mathrm{TWR-4P}}$ are the same, and they do not depend on the number of cluster nodes.

Next, SOP of the $\mathrm{TWR-4P}$ scheme can be computed as

$$\mathrm{SOP}_{\mathrm{TWR-4P}}=1-\left(1-\mathrm{OP}_1^{\mathrm{TWR-4P}}\right)\left(1-\mathrm{OP}_2^{\mathrm{TWR-4P}}\right) . \tag{14}$$

The closed-form expression of $\mathrm{SOP}_{\mathrm{TWR-4P}}$ is obtained by substituting (9)-(10) into (14).

3.1.2. IP and SIP: Firstly, considering the decoding of p_1 at E in the $\mathrm{TWR}-4\mathrm{P}$ scheme. It is worth noting that E can decode p_1 directly from S_1 or indirectly from R. Therefore, the probability of the successful decoding of p_1 at E can be formulated as

$$\begin{aligned}\chi_{p_1} &= \Pr\left(C_{\mathrm{S_1E}}^{\mathrm{TWR-4P}} < C_{\mathrm{th}}\right)\Pr\left(C_{\mathrm{S_1R}}^{\mathrm{TWR-4P}} \geq C_{\mathrm{th}}\right)\Pr\left(C_{\mathrm{RE}}^{\mathrm{TWR-4P}} \geq C_{\mathrm{th}}\right)\\ &\quad+\Pr\left(C_{\mathrm{S_1E}}^{\mathrm{TWR-4P}} \geq C_{\mathrm{th}}\right)\\ &= \exp\left(-\lambda_{\mathrm{S_1E}}\rho_{\mathrm{th1}}\right)+\left(1-\exp\left(-\lambda_{\mathrm{S_1E}}\rho_{\mathrm{th1}}\right)\right)\exp\left(-\left(\lambda_{\mathrm{S_1R}}+\lambda_{\mathrm{RE}}\right)\rho_{\mathrm{th1}}\right).\end{aligned} \tag{15}$$

Then, IP, with respect to m_1, is written as

$$\mathrm{IP}_1^{\mathrm{TWR-4P}} = \sum_{L_{\mathrm{E},1}=H_{\min}}^{N_{\max}} C_{N_{\max}}^{L_{\mathrm{E},1}}\left(\chi_{p_1}\right)^{L_{\mathrm{E},1}}\left(1-\chi_{p_1}\right)^{N_{\max}-L_{\mathrm{E},1}}. \tag{16}$$

where $L_{\mathrm{E},1}$ is the number of p_1 that E receives correctly, and m_1 is intercepted because $L_{\mathrm{E},1} \geq H_{\min}$.

Similarly, IP, with respect to m_2, in the $\mathrm{TWR}-4\mathrm{P}$ scheme is calculated as

$$\mathrm{IP}_2^{\mathrm{TWR-4P}} = \sum_{L_{\mathrm{E},2}=H_{\min}}^{N_{\max}} C_{N_{\max}}^{L_{\mathrm{E},2}}\left(\chi_{p_2}\right)^{L_{\mathrm{E},2}}\left(1-\chi_{p_2}\right)^{N_{\max}-L_{\mathrm{E},2}}, \tag{17}$$

where χ_{p_2} is the probability of the successful decoding of p_2 at E, and it is given as

$$\chi_{p_2} = \exp\left(-\lambda_{\mathrm{S_2E}}\rho_{\mathrm{th1}}\right)+\left(1-\exp\left(-\lambda_{\mathrm{S_2E}}\rho_{\mathrm{th1}}\right)\right)\exp\left(-\left(\lambda_{\mathrm{S_2R}}+\lambda_{\mathrm{RE}}\right)\rho_{\mathrm{th1}}\right). \tag{18}$$

Finally, the system intercept probability SIP in $\mathrm{TWR}-4\mathrm{P}$ is given as

$$\mathrm{SIP}_{\mathrm{TWR-4P}} = 1-\left(1-\mathrm{IP}_1^{\mathrm{TWR-4P}}\right)\left(1-\mathrm{IP}_2^{\mathrm{TWR-4P}}\right). \tag{19}$$

3.2. Performance analysis for TWR-3P

3.2.1. OP and SOP: Let V_1 denote as the number of p_1 decoded correctly by R, and $K_{2,n}$ as the number of p_1 decoded correctly by $\mathrm{S}_{2,n}$. Similar to the derivation of $\mathrm{OP}_2^{\mathrm{TWR-4P}}$, OP of the second cluster in $\mathrm{TWR}-3\mathrm{P}$ is calculated in two cases: i) $0 \leq V_1 < H_{\min}$ (denoted by $\mathrm{OP}_{2,\mathrm{TH1}}^{\mathrm{TWR-3P}}$); ii) $H_{\min} \leq V_1 \leq N_{\max}$ (denoted by $\mathrm{OP}_{2,\mathrm{TH2}}^{\mathrm{TWR-3P}}$). Indeed, $\mathrm{OP}_2^{\mathrm{TWR-3P}}$ can be written as follows

$$\begin{aligned}\mathrm{OP}_2^{\mathrm{TWR-3P}} &= \mathrm{OP}_{2,\mathrm{TH1}}^{\mathrm{TWR-3P}}+\mathrm{OP}_{2,\mathrm{TH2}}^{\mathrm{TWR-3P}}\\ &= \sum_{V_1=0}^{H_{\min}-1} C_{N_{\max}}^{V_1}\exp\left(-V_1\lambda_{\mathrm{S_1R}}\rho_{\mathrm{th2}}\right)\left[1-\exp\left(-\lambda_{\mathrm{S_1R}}\rho_{\mathrm{th2}}\right)\right]^{N_{\max}-V_1}\\ &\quad+\sum_{V_1=H_{\min}}^{N_{\max}} C_{N_{\max}}^{V_1}\exp\left(-V_1\lambda_{\mathrm{S_1R}}\rho_{\mathrm{th2}}\right)\left[1-\exp\left(-\lambda_{\mathrm{S_1R}}\rho_{\mathrm{th2}}\right)\right]^{N_{\max}-V_1}\\ &\quad\times\left\{\sum_{K_{2,n}=0}^{H_{\min}-1} C_{V_1}^{K_{2,n}}\exp\left(-K_{2,n}\lambda_{\mathrm{RS_2}}\rho_{\mathrm{th2}}\right)\left[1-\exp\left(-\lambda_{\mathrm{RS_2}}\rho_{\mathrm{th2}}\right)\right]^{V_1-K_{2,n}}\right\}^N.\end{aligned} \tag{20}$$

where $\rho_{\mathrm{th2}} = \frac{2^{3C_{\mathrm{th}}-1}}{\Delta}$.

With the same manner, OP of the first cluster is calculated as

$$\begin{aligned}
&\mathrm{OP}_1^{\mathrm{TWR-3P}} = \sum_{V_2=0}^{H_{\min}-1} C_{N_{\max}}^{V_2} \exp\left(-V_2\lambda_{\mathrm{S_2R}}\rho_{\mathrm{th2}}\right)\left[1-\exp\left(-\lambda_{\mathrm{S_2R}}\rho_{\mathrm{th2}}\right)\right]^{N_{\max}-V_2} \\
&+\sum_{V_2=H_{\min}}^{N_{\max}} C_{N_{\max}}^{V_2} \exp\left(-V_2\lambda_{\mathrm{S_2R}}\rho_{\mathrm{th2}}\right)\left[1-\exp\left(-\lambda_{\mathrm{S_2R}}\rho_{\mathrm{th2}}\right)\right]^{N_{\max}-V_2} \\
&\times\left\{\sum_{K_{1,k}=0}^{H_{\min}-1} C_{V_2}^{K_{1,k}} \exp\left(-K_{1,k}\lambda_{\mathrm{RS_1}}\rho_{\mathrm{th2}}\right)\left[1-\exp\left(-\lambda_{\mathrm{RS_1}}\rho_{\mathrm{th2}}\right)\right]^{V_2-K_{1,k}}\right\}^M .
\end{aligned} \tag{21}$$

Moreover, the approximate expressions of $\mathrm{OP}_1^{\mathrm{TWR-3P}}$ and $\mathrm{OP}_2^{\mathrm{TWR-3P}}$ at the high can be computed, respectively as

$$\begin{aligned}
\mathrm{OP}_1^{\mathrm{TWR-3P}} &\overset{\Delta\to+\infty}{\approx} C_{N_{\max}}^{H_{\min}-1}\left(\lambda_{\mathrm{S_2R}}\rho_{\mathrm{th2}}\right)^{N_{\max}+1-H_{\min}}, \\
\mathrm{OP}_2^{\mathrm{TWR-3P}} &\overset{\Delta\to+\infty}{\approx} C_{N_{\max}}^{H_{\min}-1}\left(\lambda_{\mathrm{S_1R}}\rho_{\mathrm{th2}}\right)^{N_{\max}+1-H_{\min}}.
\end{aligned} \tag{22}$$

Hence, $\mathrm{OP}_1^{\mathrm{TWR-3P}}$ and $\mathrm{OP}_2^{\mathrm{TWR-3P}}$ have the same slope, i.e.,

$$\mathrm{D}_1^{\mathrm{TWR-3P}} = \mathrm{D}_2^{\mathrm{TWR-3P}} = N_{\max} + 1 - H_{\min}. \tag{23}$$

The (12), (13), and (23) show that the slopes of $\mathrm{OP}_1^{\mathrm{TWR-4P}}$, $\mathrm{OP}_2^{\mathrm{TWR-4P}}$, $\mathrm{OP}_1^{\mathrm{TWR-3P}}$, and $\mathrm{OP}_2^{\mathrm{TWR-3P}}$ are the same, and equal $N_{\max} + 1 - H_{\min}$.

Next, SOP of the $\mathrm{TWR-3P}$ scheme is given as

$$\mathrm{SOP}_{\mathrm{TWR-3P}} = 1 - \left(1-\mathrm{OP}_1^{\mathrm{TWR-3P}}\right)\left(1-\mathrm{OP}_2^{\mathrm{TWR-3P}}\right). \tag{24}$$

Substituting (20)-(21) into (24) obtains an exact expression of $\mathrm{SOP}_{\mathrm{TWR-3P}}$.

3.2.2. IP and SIP: At first, calculating probability of the successful decoding of p_1 at E in the $\mathrm{TWR-3P}$ scheme exactly as follows

$$\begin{aligned}
\theta_{p_1} &= \Pr\left(C_{\mathrm{S_1E}}^{\mathrm{TWR-3P}} < C_{\mathrm{th}}\right)\Pr\left(C_{\mathrm{S_1R}}^{\mathrm{TWR-3P}} \ge C_{\mathrm{th}}\right)\Pr\left(C_{\mathrm{RE}}^{\mathrm{TWR-3P}} \ge C_{\mathrm{th}}\right) \\
&\quad + \Pr\left(C_{\mathrm{S_1E}}^{\mathrm{TWR-3P}} \ge C_{\mathrm{th}}\right) \\
&= \exp\left(-\lambda_{\mathrm{S_1E}}\rho_{\mathrm{th2}}\right) + \left(1-\exp\left(-\lambda_{\mathrm{S_1E}}\rho_{\mathrm{th2}}\right)\right)\exp\left(-\left(\lambda_{\mathrm{S_1R}}+\lambda_{\mathrm{RE}}\right)\rho_{\mathrm{th2}}\right).
\end{aligned} \tag{25}$$

Next, IP, with respect to the data m_1, in $\mathrm{TWR-3P}$ is written as

$$\mathrm{IP}_1^{\mathrm{TWR-3P}} = \sum_{L_{\mathrm{E},1}=H_{\min}}^{N_{\max}} C_{N_{\max}}^{L_{\mathrm{E},1}}\left(\theta_{p_1}\right)^{L_{\mathrm{E},1}}\left(1-\theta_{p_1}\right)^{N_{\max}-L_{\mathrm{E},1}}. \tag{26}$$

Similarly, IP, with respect to the data m_2, is expressed as

$$\mathrm{IP}_2^{\mathrm{TWR-3P}} = \sum_{L_{\mathrm{E},2}=H_{\min}}^{N_{\max}} C_{N_{\max}}^{L_{\mathrm{E},2}}\left(\theta_{p_2}\right)^{L_{\mathrm{E},2}}\left(1-\theta_{p_2}\right)^{N_{\max}-L_{\mathrm{E},2}}. \tag{27}$$

where $\theta_{p_2} = \exp\left(-\lambda_{\mathrm{S_2E}}\rho_{\mathrm{th2}}\right) + \left(1-\exp\left(-\lambda_{\mathrm{S_2E}}\rho_{\mathrm{th2}}\right)\right)\exp\left(-\left(\lambda_{\mathrm{S_2R}}+\lambda_{\mathrm{RE}}\right)\rho_{\mathrm{th2}}\right).$

For SIP in the $\mathrm{TWR-3P}$ scheme, $\mathrm{SIP}_{\mathrm{TWR-3P}}$ can be written

$$\mathrm{SIP}_{\mathrm{TWR-3P}} = 1 - \left(1 - \mathrm{IP}_1^{\mathrm{TWR-3P}}\right)\left(1 - \mathrm{IP}_2^{\mathrm{TWR-3P}}\right). \tag{28}$$

Substituting (26)-(27) into (28) obtains an exact closed-form formula of $\mathrm{SIP}_{\mathrm{TWR-3P}}$.

4. Simulation results

This section provides Monte Carlo simulations to validate the correctness of the expressions given in Section 3. In the 2D coordinate Oxy, the nodes of the first cluster, the nodes of the second cluster, R, and E are placed in the positions $(0,0)$, $(x_{\mathrm{R}},0)$, and $(0.5,0.75)$ respectively, where $(0 < x_{\mathrm{R}} < 1)$. Additionally, the other system parameters are also fixed in all the simulations such as $\beta = 3$, $\sigma_0^2 = 1$, $C_{\mathrm{th}} = 1$, and $H_{\min} = 5$.

Fig. 2a and Fig. 2b show OP and IP of two proposed schemes as a function of Δ(dB) when $M = 3$, $N = 5$, $x_{\mathrm{R}} = 0.4$, and $N_{\max} = 6$. Firstly, it is clear that the simulation results (MP) match well with the exactly analytical ones $(\mathrm{LT-CS})$. In Fig. 2a, the MP and $\mathrm{LT-CS}$ result converge to the asymptoticly theoretical ones $(\mathrm{LT-TC})$ at high Δ while the $\mathrm{OP}_1^{\mathrm{TWR-4P}}, \mathrm{OP}_2^{\mathrm{TWR-4P}}, \mathrm{OP}_1^{\mathrm{TWR-3P}}$ and $\mathrm{OP}_2^{\mathrm{TWR-3P}}$ have the same slope as proved in Section 3. Next, as seen in Fig. 2a and Fig. 2b, when Δ increases, the value of OP decreases, but that of IP increases. Furthermore, OP performance of $\mathrm{TWR-4P}$ is worse than that of $\mathrm{TWR-3P}$, but IP with respect to the data $m_1(m_2)$ of $\mathrm{TWR-4P}$ is lower than that of $\mathrm{TWR-3P}$. Therefore, these results show a trade-off between OP and IP.

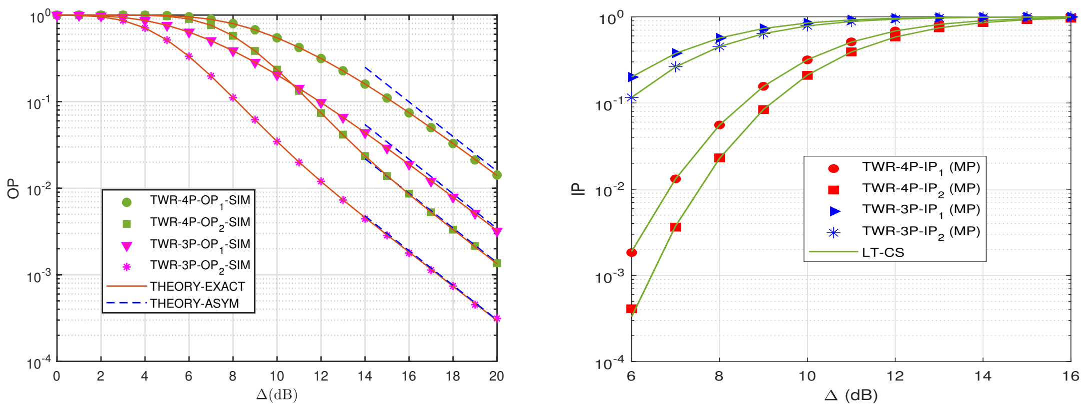

(a) OP as a function of $\Delta(dB)$ *(b) IP as a function of $\Delta(dB)$*

Fig. 2. OP and IP as functions of $\Delta(dB)$ when $M = 3$, $N = 5$, $x_{\mathrm{R}} = 0.4$, and $N_{\max} = 6$.

Fig. 3a and Fig. 3b investigate the impact of $N_{\max}$ on the OP and IP performance of two proposed schemes when $M = 7$, $N = 5$, $x_{\mathrm{R}} = 0.6$, and $\Delta = 6$ (dB). Again, the MP results validate the $\mathrm{LT-CS}$ ones. Next, OP(IP) in the $\mathrm{TWR-3P}$ scheme is significantly lower (higher) than OP(IP) in the $\mathrm{TWR-4P}$ scheme. Furthermore,

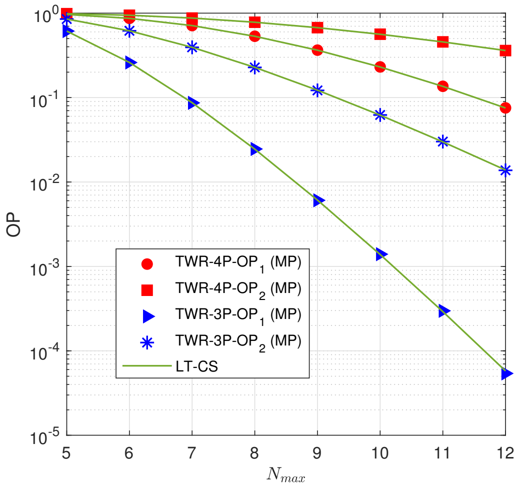

(a) OP as a function of $N_{\max}$

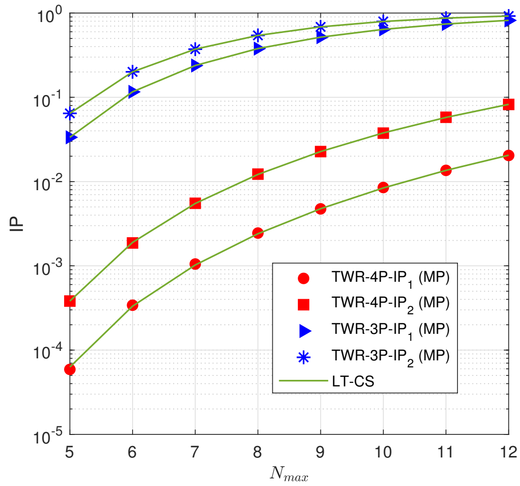

(b) IP as a function of $N_{\max}$

Fig. 3. OP and IP as functions of $N_{\max}$ when $M = 7$, $N = 5$, $x_{\mathrm{R}} = 0.6$, and $\Delta = 6$ (dB).

when $N_{\max}$ increases, OP(IP) in two schemes decreases (increases) because the nodes have more opportunity to sufficiently receive $H_{\min}$ encoded packets. Hence, Fig. 3a and Fig. 3b show the OP-IP trade-off, with respect to $N_{\max}$.

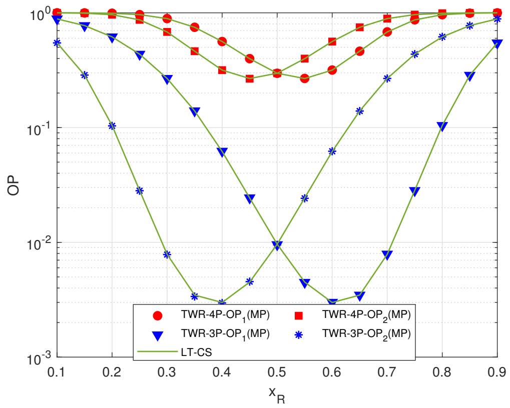

(a) OP as a function of x_{R}

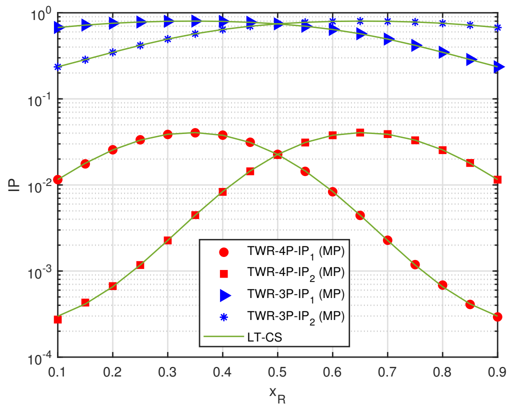

(b) IP as a function of x_{R}

Fig. 4. OP and IP as functions of x_{R} when $\Delta = 6(dB)$, $M = 5$, $N = 5$, and $N_{\max} = 10$.

Fig. 4a and Fig. 4b present OP and IP of the proposed schemes as a function of x_{R} when $M = 5$, $N = 5$, $N_{\max} = 10$, and $\Delta = 6$ (dB). Obviously, both the OP and IP performance are effected significantly by the positions of R. As can be seen from Fig. 4a, if R is located near the first cluster or the second cluster, the OP values are very high. Moreover, OP achieves the lowest value at $x_{\mathrm{R}} = 0.55$ or $x_{\mathrm{R}} = 0.45$ in $\mathrm{TWR} - 4\mathrm{P}$, and at $x_{\mathrm{R}} = 0.6$ or $x_{\mathrm{R}} = 0.4$ in $\mathrm{TWR} - 3\mathrm{P}$. Especially, when $x_{\mathrm{R}} = 0.5$, OP of two proposed schemes are the same. In Fig. 4b, IP in $\mathrm{TWR-3P}$ and $\mathrm{TWR-4P}$ change with different values of x_{R}. Indeed, if R is near E, the overhearing possibility of E increases, and vice versa. It is also seen from Fig. 4b that IP in both the schemes are the same value as $x_{\mathrm{R}} = 0.5$.

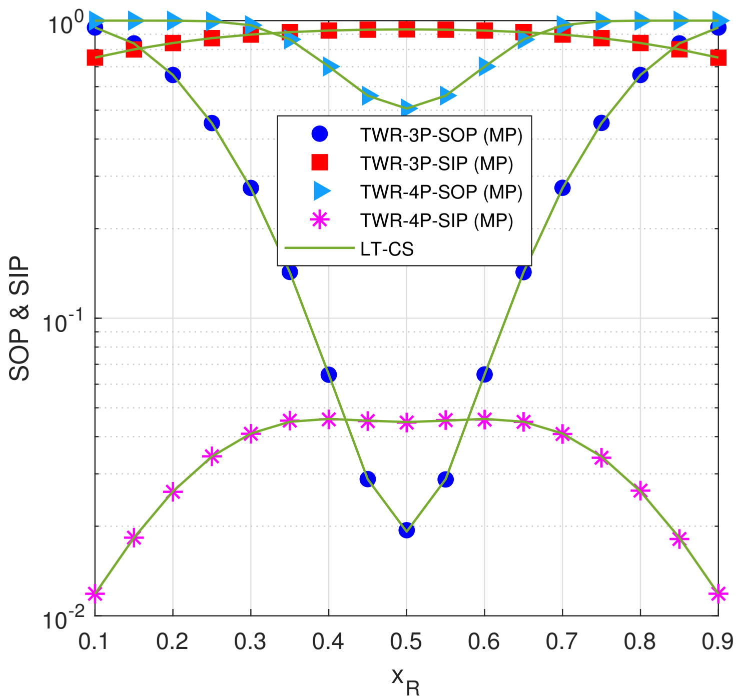

Fig. 5. SOP and SIP as a function of x_{R} when $M = 5$, $N = 5$, $\Delta = 6$ (dB), and $N_{\max} = 10$.

Fig. 5 investigates the impact of x_{R} on SOP and SIP of the proposed scheme when $M = 5$, $N = 5$, $\Delta = 6$ (dB), and $N_{\max} = 10$. We can observe that SOP of $\mathrm{TWR-3P}$ is lower than that of $\mathrm{TWR-4P}$, but SIP in $\mathrm{TWR-3P}$ is higher. Fig. 5 also presents that the SOP performance of $\mathrm{TWR-3P}$ and $\mathrm{TWR-4P}$ is best as $x_{\mathrm{R}} = 0.5$. For SIP, the proposed schemes obtain better SIP performance as R locates near one of two clusters. It is also seen from Fig. 5 that there exists the SOP-SIP trade-off, with respect to the position of the relay R.

Fig. 6 presents the SOP-SIP trade-off by presenting SIP as a function of SOP. In this figure, the parameters are set as follows: $M = 5$, $N = 5$, and $N_{\max} = 10$. As seen from Fig. 6, to obtain better SOP performance, the proposed schemes receive worse SIP performance. Moreover, with the same SOP values, it is seen that the SIP values of the $\mathrm{TWR-3P}$ and $\mathrm{TWR-4P}$ schemes are almost same. This means that $\mathrm{TWR-3P}$ and $\mathrm{TWR-4P}$ have the same SOP-SIP trade-off performance. It is also observed that, as x_{R} increases from 0.35 to 0.5, the SOP-SIP trade-off performance of the proposed schemes is better. Therefore, the Fig. 5 and Fig. 6 show that with respect to the SOP and SOP-SIP trade-off performance, $x_{\mathrm{R}} = 0.5$ is the optimal position of R.

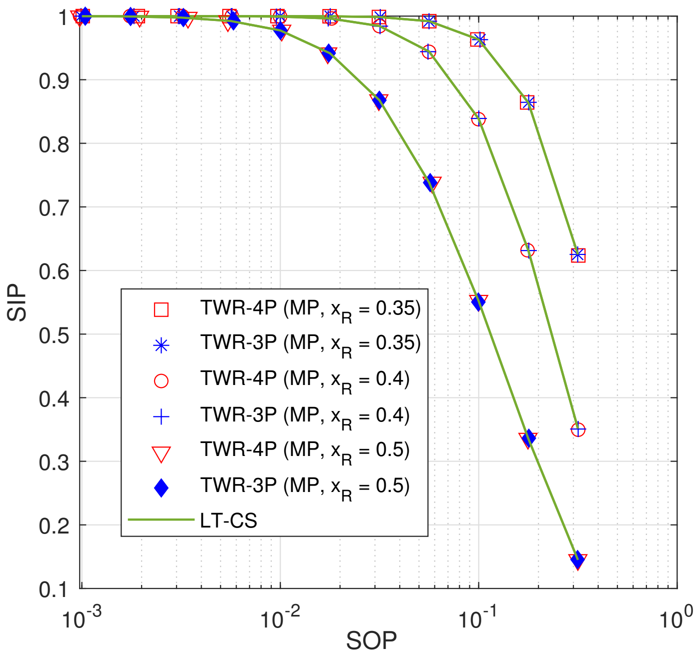

Fig. 6. SIP as a function of SOP when $M = 5$, $N = 5$, and $N_{\max} = 10$.

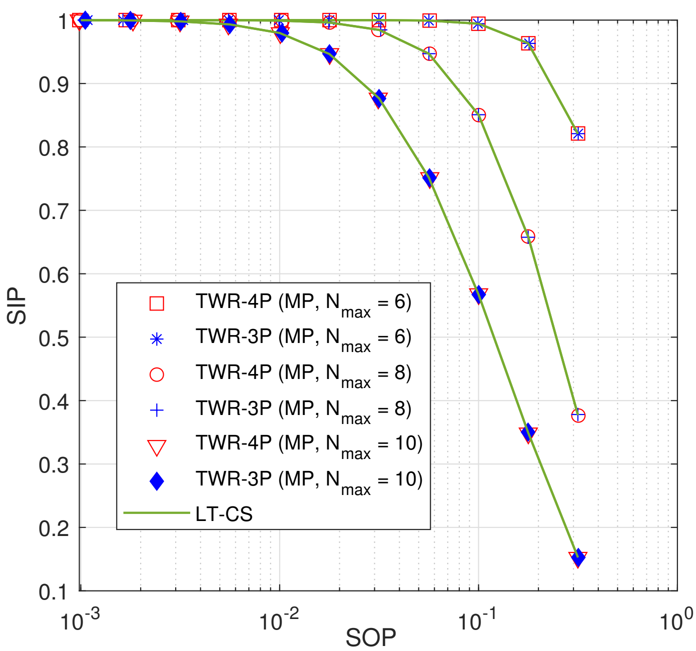

Fig. 7. SIP as a function of SOP when $M = 4$, $N = 6$, and $x_{\mathrm{R}} = 0.5$.

Fig. 7 presents SIP as a function of SOP-SIP with the different values of $N_{\max}$ when $M = 4$, $N = 6$, and $x_{\mathrm{R}} = 0.5$. Similar to Fig. 6, there exists a trade-off between SOP and SIP, and SIP in two proposed schemes is the same at the same SOP value. As seen from Fig. 7, the SOP-SIP trade-off performance is better as increasing $N_{\max}$. However, it is worth noting that increasing $N_{\max}$ also increases delay time and energy consumption. Therefore, the value of $N_{\max}$ needs to be designed carefully.

5. Conclusions

This paper proposed two TWR-PLS schemes between two clusters of nodes using FCs, and evaluated the OP(SOP) and IP(SIP) performance of the proposed schemes through analysis and computer simulations. In addition, the approximate expressions of OP at high SNR regions were provided, and it was demonstrated that OP of the clusters in both the proposed schemes have the same slope. The results presented a trade-off between reliability (OP and SOP) and security (IP and SIP), according to the transmission power of the nodes, the maximum number of transmissions, and the position of the relay node. In the case of a symmetric network, the relay node located in the middle of the two clusters will achieve the optimal SOP and SOP-SIP trade-off performance. The paper also showed that the two proposed schemes have the same SOP-SIP trade-off performance, and this trade-off is significantly affected by the position of the relay and the maximum number of transmission times.

In the future, our proposed schemes will be extended to multi-antenna nodes utilizing emerging technologies such as radio-frequency energy harvesting and cognitive radio. Furthermore, we will analyze the performance of the proposed schemes over generalized fading channels, such as Rician and Nakagami-m.

Acknowledgements

This research is funded by Vietnam National Foundation for Science and Technology Development (NAFOSTED) under grant number 102.04-2021.57.

References

[1] T. T. Duy and H. Y. Kong, "Exact outage probability of cognitive two-way relaying scheme with opportunistic relay selection under interference constraint," *IET Communications*, vol. 6, no. 16, pp. 2750–2759, 2012, DOI: 10.1049/iet-com.2012.0235

[2] P. N. Son and H. Y. Kong, "Exact outage probability of two-way decode-and-forward scheme with opportunistic relay selection under physical-layer security," *Wireless Personal Communications*, vol. 77, pp. 2889–2917, 2014, DOI: 10.1007/s11277-014-1674-6

[3] T.-T. T. Dao and P. N. Son, "Two-way SWIPT relaying networks with nonlinear power splitting, digital network coding and selection combining," *Wireless Personal Communications*, vol. 133, no. 4, pp. 2445–2465, 2023, DOI: 10.1007/s11277-024-10882-1

[4] P. N. Son and T. T. Duy, "A new approach for two-way relaying networks: improving performance by successive interference cancellation, digital network coding and opportunistic relay selection," *Wireless Networks*, vol. 26, no. 2, pp. 1315–1329, 2020, DOI: 10.1007/s11276-019-02186-1

[5] G. Zheng, "Joint beamforming optimization and power control for full-duplex MIMO two-way relay channel," *IEEE Transactions on Signal Processing*, vol. 63, no. 3, pp. 555–566, 2015, DOI: 10.1109/TSP.2014.2376885

[6] P. Nguyen-Huu, K. Ho-Van, and V. N. Q. Bao, "Evaluating the effect of self-interference on the performance of full-duplex two-way relaying communication with energy harvesting," *REV Journal on Electronics and Communications*, vol. 9, no. 3-4, 2019, DOI: 10.21553/rev-jec.240

[7] W. Trappe, "The challenges facing physical-layer security," *IEEE communications magazine*, vol. 53, no. 6, pp. 16–20, 2015, DOI: 10.1109/MCOM.2015.7120011

[8] M. Mitev, A. Chorti, H. V. Poor, and G. P. Fettweis, "What physical-layer security can do for 6G security," *IEEE Open Journal of Vehicular Technology*, vol. 4, pp. 375–388, 2023, DOI: 10.1109/OJVT.2023.3245071

[9] J. Mo, M. Tao, and Y. Liu, "Relay placement for physical-layer security: A secure connection perspective," *IEEE Communications Letters*, vol. 16, no. 6, pp. 878–881, 2012, DOI: 10.1109/LCOMM.2012.042312.120582

[10] D.-H. Ha, T. T. Duy, P. N. Son, T. Le-Tien, and M. Voznak, "Security-reliability trade-off analysis for rateless codes-based relaying protocols using NOMA, cooperative jamming and partial relay selection," *IEEE Access*, vol. 9, pp. 131 087–131 108, 2021, DOI: 10.1109/ACCESS.2021.3114343

[11] P. M. Nam, P. N. Dinh, N. L. Nhat, T. Lam-Thanh, and T. Le-Tien, "On the performance of the relay selection in multi-hop cluster-based wireless networks with multiple eavesdroppers under equally correlated Rayleigh fading," *EAI Endorsed Transactions on Industrial Networks and Intelligent Systems*, vol. 11, no. 3, 2024, DOI: 10.4108/eetinis.v11i3.4728

[12] K. Pärlin, T. Riihonen, M. Turunen, V. Le Nir, and M. Adrat, "Known-interference cancellation in cooperative jamming: Experimental evaluation and benchmark algorithm performance," *IEEE Wireless Communications Letters*, vol. 12, no. 9, pp. 1598–1602, 2023, DOI: 10.1109/LWC.2023.3284006

[13] C. Gao, B. Yang, D. Zheng, X. Jiang, and T. Taleb, "Cooperative jamming and relay selection for covert communications in wireless relay systems," *IEEE Transactions on Communications*, vol. 72, no. 2, pp. 1020–1032, 2023, DOI: 10.1109/TCOMM.2023.3327272

[14] P. N. Son and H. Y. Kong, "An integration of source and jammer for a decode-and-forward two-way scheme under physical-layer security," *Wireless Personal Communications*, vol. 79, pp. 1741–1764, 2014, DOI: 10.1007/s11277-014-1956-z

[15] J. Luo, F. Wang, and S. Wang, "Secure two-way transmission via autonomous reconfigurable intelligent surface," *IEEE Wireless Communications Letters*, vol. 12, no. 2, pp. 262–266, 2022, DOI: 10.1109/LWC.2022.3223345

[16] Y. Zhang, S. Zhao, Y. Shen, X. Jiang, and N. Shiratori, "Enhancing the physical-layer security of two-way relay systems with RIS and beamforming," *IEEE Transactions on Information Forensics and Security*, vol. 19, pp. 5696–5711, 2024, DOI: 10.1109/TIFS.2024.3402373

[17] A. Shokrollahi, "Raptor codes," *IEEE Transactions on Information Theory*, vol. 52, no. 6, pp. 2551–2567, 2006, DOI: 10.1109/TIT.2006.874390

[18] L.-T. Tu, T. N. Nguyen, T. T. Duy, P. T. Tran, M. Voznak, and A. I. Aravanis, "Broadcasting in cognitive radio networks: A Fountain codes approach," *IEEE Transactions on Vehicular Technology*, vol. 71, no. 10, pp. 11 289–11 294, 2022, DOI: 10.1109/TVT.2022.3188969 .

[19] H. Niu, M. Iwai, K. Sezaki, L. Sun, and Q. Du, "Exploiting Fountain codes for secure wireless delivery," *IEEE Communications Letters*, vol. 18, no. 5, pp. 777–780, 2014, DOI: 10.1109/LCOMM.2014.030914.140030

[20] L. Sun, P. Ren, Q. Du, and Y. Wang, "Fountain-coding aided strategy for secure cooperative transmission in industrial wireless sensor networks," *IEEE Transactions on Industrial Informatics*, vol. 12, no. 1, pp. 291–300, 2015, DOI: 10.1109/TII.2015.2509442

[21] N. Đ. Phong, P. M. Quang, N. T. Hiếu, and T. T. Duy, "Nghiên cứu sự đánh đổi giữa bảo mật và độ tin cậy cho mạng quảng bá đa người dùng sử dụng mã Fountain trong vô tuyến lĩnh hội," *Tạp chí Khoa học công nghệ Thông tin và Truyền thông*, vol. 3, pp. 99–106, 2022.

[22] N. Q. Sang, N. V. Hien, T. T. Duy, N. L. Nhat, and L.-T. Tu, "On the security and reliability trade-off of the satellite terrestrial networks with Fountain codes and friendly jamming," *EAI Endorsed Transactions on Industrial Networks and Intelligent Systems*, vol. 10, no. 4, pp. 1–11, 2023, DOI: 10.4108/eetinis.v10i4.4192

Manuscript received 5-10-2024; Accepted 27-12-2024.

■

Thi Hau Nguyen received the B.E. degree in Electronics and Telecommunication Engineering from The University of Danang – University of Science and Technology (DUT), Vietnam in 2007 and the M.S. degree in Electronics Engineering from Ho Chi Minh City University of Technology, Vietnam in 2011. She is currently working as a lecturer in the Faculty of Electronics and Telecommunications, Saigon University (SGU) and pursuing the Ph.D. degree in the Faculty of Electronics Technology, Industrial University Ho Chi Minh City (IUH), Vietnam. Her research interests include cooperative communications, cognitive radio, energy harvesting, physical-layer security in wireless communications, and Fountain codes. Email: hau.nt@sgu.edu.vn

Minh Nam Pham was born in Thanh Hoa, Vietnam, in 1976. He graduated from Ho Chi Minh City University of Technology (HCMUT) with B.E and M.E. degree (2010), and Ho Chi Minh City University of Technology and Education (HCMUTE) with a Ph.D. degree (2022) in Electronic and Telecommunication Engineering. He has worked as a lecturer in the Faculty of Electronics Technology, Industrial University Ho Chi Minh City (IUH) since 2010. His major researches focus on energy harvesting, multi-hop network, cognitive radio, power constraint, and physical layer security in wireless communications. E-mail: phamminhnam@iuh.edu.vn

Tran Trung Duy received the B.E. degree in Electronics and Telecommunications Engineering from the French-Vietnamese training program for excellent engineers (PFIEV), Ho Chi Minh City University of Technology, Vietnam in 2007. In 2013, he received the Ph.D degree in Electrical Engineering from University of Ulsan, South Korea. In 2013, he joined Posts and Telecommunications Institute of Technology, Ho Chi Minh City campus (PTIT-HCM), as a lecturer. From 2022, he is an associate Professor of Wireless Communications at PTIT-HCM. His major research interests are cooperative communications, cooperative multi-hop, cognitive radio, physical-layer security, energy harvesting, hardware impairments and Fountain codes. E-mail: trantrungduy@ptithcm.edu.vn.

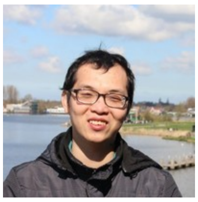

Lam-Thanh Tu received the B.Eng. degree in Electronics and Telecommunications Engineering from the Ho Chi Minh City University of Technology, Vietnam, in 2009, the M.Sc. degree in Telecommunications Engineering from the Posts and Telecommunications Institute of Technology, Vietnam, in 2014, and the Ph.D. degree from the University of Paris Sud (Paris-Saclay University), France, in 2018. From 2015 to 2018, he was with the French National Center for Scientific Research (CNRS), Paris, as an Early Stage Researcher of the European-Funded Project H2020 ETN-5Gwireless. From 2019 to 2021, he was with the Xlim Research Institute, University of Poitiers, France, as a Post-Doctoral Research Fellow. Since 2022, he has been with the Faculty of Electrical and Electronics Engineering, Ton Duc Thang University, Vietnam. His research interests include stochastic geometry, LoRa networks, reconfigurable intelligent surfaces, covert communications, and artificial intelligence applications for wireless communications. He was a recipient of the 2017 IEEE SigTelCom and the 2022 RICE Best Paper Award. He has been a member of the Technical Program Committee of several conferences, such as IEEE Globecom, IEEE ICC, IEEE SPAWC, EuCNC, IEEE ATC, and IEEE NICS. He was an IEEE Transactions on Communications exemplary reviewer in 2016. Since 2023, he has been an Associate Editor of the IEEE Communications Letters and the Managing Editor of the Advances in Electrical and Electronic Engineering. E-mail: tulamthanh@tdtu.edu.vn.

Van Khuong Ho received the B.E. (first-rank Hons.) and M.S. degrees in Electronics and Telecommunications Engineering from Ho Chi Minh City University of Technology, Ho Chi Minh City, Vietnam, in 2001 and 2003, respectively, and the Ph.D. degree in Electrical Engineering from the University of Ulsan, Ulsan, South Korea, in 2007. He joined McGill University, Montreal, QC, Canada, as a Post-Doctoral Research Fellow from 2007 to 2011. He is currently an Associate Professor with Ho Chi Minh City University of Technology. His major research interests are modulation and coding techniques, diversity techniques, digital signal processing, energy harvesting, physical-layer security, and cognitive radio. E-mail: hvkhuong@hcmut.edu.vn.

PHÂN TÍCH SỰ ĐÁNH ĐỔI HIỆU NĂNG XÁC SUẤT DỪNG VÀ XÁC SUẤT CHẶN CHO CÁC MÔ HÌNH CHUYỂN TIẾP HAI CHIỀU BẢO MẬT GIỮA HAI CỤM NÚT SỬ DỤNG MÃ FOUNTAIN

Nguyễn Thị Hậu, Phạm Minh Nam, Trần Trung Duy, Từ Lâm Thanh, Hồ Văn Khương

Tóm tắt

Bài báo này nghiên cứu hai mô hình mạng bảo mật chuyển tiếp hai chiều giữa hai cụm nút: 1) chuyển tiếp hai chiều 3 pha sử dụng mã hóa mạng số (Digital Network Coding), 2) chuyển tiếp hai chiều 4 pha. Sử dụng mã Fountain, một nút được chọn trong mỗi cụm sẽ mã hóa thông tin gốc và gửi các gói mã hóa đến các cụm còn lại với sự trợ giúp của một nút chuyển tiếp trung gian. Bài báo đưa ra các biểu thức toán học để đánh giá xác suất dừng (xác suất dừng hệ thống) và xác suất chặn (xác suất chặn hệ thống) đối với các dữ liệu được gửi đi từ mỗi cụm. Tất cả các biểu thức đưa ra đều được kiểm chứng sự chính xác qua mô phỏng Monte Carlo. Các kết quả đạt được cho thấy có sự đánh đổi giữa độ tin cậy dữ liệu và sự bảo mật thông tin. Cuối cùng, sự tác động của các tham số hệ thống lên các hiệu năng mạng được phân tích kỹ trong nghiên cứu này.

Từ khóa

Chuyển tiếp hai chiều; mã hóa mạng số; bảo mật lớp vật lý; mã Fountain; xác suất dừng; xác suất chặn.